Gel-shift assays

p73α, p73α (R293H) or ΔN-p73α cDNA containing pcDNA-3 were transcribed and subsequently *in vitro* translated using TNT7-coupled reticulocyte lysate system (Promega). Each DNA-binding reaction contained 2.5 μl of reticulocyte lysate, 2.5 mM of DDT, 10 ng of ^{32}P-labelled DNA, 1 μg of salmon DNA as non-specific competitor, 12. μl of glycerol and Tris-buffered saline (TBS; 25 mM Tris pH 7.5, 130 mM NaCl, 3 mM KCl) to 10 μl final volume. Reactions were incubated at 23 °C for 30 min, cooled to 4 °C and electrophoresed in 4% non-denaturing polyacrylamide gel in a low salt buffer (0.4 × TBE).

1. Kaghad, M. *et al.* Monoallelically expressed gene related to p53 at 1p36, a region frequently deleted in neuroblastoma and other human cancers. *Cell* **90**, 809–819 (1997).
2. Kinzler, K. W. & Vogelstein, B. Life (and death) in a malignant tumour. *Nature* **379**, 19–20 (1996).
3. Ko, L. J. & Prives, C. p53: puzzle and paradigm. *Genes Dev.* **10**, 1054–1072 (1996).
4. Levine, A. J. p53, the cellular gatekeeper for growth and division. *Cell* **88**, 323–331 (1997).
5. Yang, A. *et al.* p63, a p53 homolog at 3q27-29, encodes multiple products with transactivating, death-inducing, and dominant-negative activities. *Mol. Cell* **2**, 305–316 (1998).
6. Yang, A. *et al.* p63 is essential for regenerative proliferation in limb, craniofacial and epithelial development. *Nature* **398**, 714–718 (1999).
7. Mills, A. A. *et al.* p63 is a p53 homologue required for limb and epidermal morphogenesis. *Nature* **398**, 708–713 (1999).
8. De Laurenzi, V. *et al.* Two new p73 splice variants, gamma and delta, with different transcriptional activity. *J. Exp. Med.* **188**, 1763–1768 (1998).
9. Capecchi, M. R. Altering the genome by homologous recombination. *Science* **244**, 1288–1292 (1989).
10. Li, E., Bestor, T. H. & Jaenisch, R. Targeted mutation of the DNA methyltransferase gene results in embryonic lethality. *Cell* **69**, 915–926 (1992).
11. Donehower, L. A. Mice deficient for p53 are developmentally normal but susceptible to spontaneous tumours. *Nature* **356**, 215–221 (1992).
12. Jacks, T. *et al.* Tumor spectrum analysis in p53-mutant mice. *Curr. Biol.* **4**, 1–7 (1994).
13. Kim, K. C. *et al.* Airway goblet cell mucin: its structure and regulation of secretion. *Eur. Respir. J.* **10**, 2644–2649 (1997).
14. Matsui, H. *et al.* Evidence for periciliary liquid layer depletion, not abnormal ion composition, in the pathogenesis of cystic fibrosis airways disease. *Cell* **95**, 1005–1015 (1998).
15. Cressman, V. L., Hicks, E. M., Funkhouser, W. K., Backlund, D. C. & Koller, B. H. The relationship of chronic mucin secretion to airway disease in normal and CFTR-deficient mice. *Am. J. Respir. Cell. Mol. Biol.* **19**, 853–866 (1998).
16. Go, K. G. The normal and pathological physiology of brain water. *Adv. Tech. Stand. Neurosurg.* **23**, 47–142 (1997).
17. Lindeman, G. J. A specific, nonproliferative role for E2F-5 in choroid plexus function revealed by gene targeting. *Genes Dev.* **12**, 1092–1098 (1998).
18. Stanfield, B. B. & Cowan, W. M. The morphology of the hippocampus and dentate gyrus in normal and Reeler mice. *J. Comp. Neurol.* **185**, 393–422 (1979).
19. Rakic, P. & Caviness, V. S. Jr Cortical development: view from neurological mutants two decades later. *Neuron* **14**, 1101–1104 (1995).
20. Ogawa, M. *et al.* The reeler gene-associated antigen on Cajal–Retzius neurons is a crucial molecule for laminar organization of cortical neurons. *Neuron* **14**, 899–912 (1995).
21. D'Arcangelo, G. *et al.* A protein related to extracellular matrix proteins deleted in the mouse mutant reeler. *Nature* **374**, 719–723 (1995).
22. Frotscher, M. Cajal–Retzius cells, Reelin, and the formation of layers. *Curr. Opin. Neurobiol.* **8**, 570–575 (1998).
23. D'Arcangelo, G. & Curran, T. Reeler: new tales on an old mutant mouse. *BioEssays* **20**, 235–244 (1998).
24. Alcantara, S. *et al.* Regional and cellular patterns of reelin mRNA expression in the forebrain of the developing and adult mouse. *J. Neurosci.* **18**, 7779–7799 (1998).
25. McEwen, B. S. Stress and hippocampal plasticity. *Annu. Rev. Neurosci.* **22**, 105–122 (1999).
26. Gage, F. H., Kempermann, G., Palmer, T. D., Peterson, D. A., Ray, J. Multipotent progenitor cells in the adult dentate gyrus. *J. Neurobiol.* **36**, 249–266 (1998).
27. Bargmann, C. I. Olfactory receptors, vomeronasal receptors, and the organization of olfactory information. *Cell* **90**, 585–587 (1997).
28. Tirindelli, R. & Mucignat-Caretta, C., Ryba, N. J. Molecular aspects of pheromonal communication via the vomeronasal organ of mammals. *Trends Neurosci.* **21**, 482–486 (1998).
29. Matsunami, H. & Buck, L. A multigene family encoding a diverse array of putative pheromone receptors in mammals. *Cell* **90**, 775–784 (1997).
30. Herrada, G. & Dulac, C. A novel family of putative pheromone receptors in mammals with a topographically organized and sexually dimorphic distribution. *Cell* **90**, 763–773 (1997).

··

Single-molecule studies of the effect of template tension on T7 DNA polymerase activity

Gijs J.L. Wuite*, **Steven B. Smith***, **Mark Young**†, **David Keller**‡ **& Carlos Bustamante***

* *Department of Physics and Department of Molecular and Cell Biology, University of California, Berkeley, California 94720, USA*
† *Institute of Molecular Biology, University of Oregon, Eugene, Oregon 97403, USA*
‡ *Department of Chemistry, University of New Mexico, Albuquerque, New Mexico 87131, USA*

··

T7 DNA polymerase[1,2] catalyses DNA replication *in vitro* at rates of more than 100 bases per second and has a 3′→5′ exonuclease (nucleotide removing) activity at a separate active site. This enzyme possesses a 'right hand' shape which is common to most polymerases with fingers, palm and thumb domains[3,4]. The rate-limiting step for replication is thought to involve a conformational change between an 'open fingers' state in which the active site samples nucleotides, and a 'closed' state in which nucleotide incorporation occurs[3,5]. DNA polymerase must function as a molecular motor converting chemical energy into mechanical force as it moves over the template. Here we show, using a single-molecule assay based on the differential elasticity of single-stranded and double-stranded DNA, that mechanical force is generated during the rate-limiting step and that the motor can work against a maximum template tension of
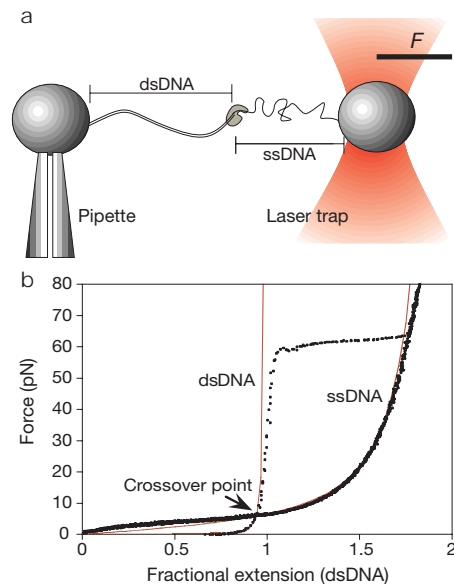

Figure 1 Optical trap setup. **a**, A 10,416-base pair plasmid DNA fragment was prepared as described[18] and attached between two beads, one held on the tip of a glass pipette, the other in an optical trap. Single-stranded DNA was obtained by using the force-induced exonuclease activity of T7 DNAp to remove any desired length of the non-template strand. The end-to-end length of the DNA was obtained by video imaging of the bead positions, and the force (F) was measured using the change in light momentum which exits the dual-beam trap[6]. **b**, Force–extension data for dsDNA and ssDNA (dotted lines), compared with the wormlike chain model using ssDNA and dsDNA persistence lengths of 0.7 nm and 53 nm respectively (solid lines)[7,8]. Difference between ssDNA and WLC curves at low tension is due to partial hairpin formation and disappears if magnesium is removed from buffer.

103

~34 pN. **Estimates of the mechanical and entropic work done by the enzyme show that T7 DNA polymerase organizes two template bases in the polymerization site during each catalytic cycle. We also find a force-induced 100-fold increase in exonucleolysis above 40 pN.**

We measured T7 DNA polymerase (DNAp) activity by using the optical-trap shown in Fig. 1a[6]. Because single-stranded (ss) and double-stranded (ds) DNA differ in length at any given tension[6–8] (Fig. 1b), conversion between these two forms changes the molecule's tension if the end-to-end distance of the template is held constant. Alternatively, the molecule's end-to-end distance changes if the tension is held constant. The end-to-end distance of ssDNA (Fig. 1b) is shorter than that of dsDNA for tensions below 6.5 pN ('crossover point') because ssDNA, despite having about twice the contour length of dsDNA, is more retractile owing to its greater flexibility. Above 6.5 pN, however, contour length predominates over entropy and ssDNA is longer than dsDNA. The force–extension curve of a molecule that is partly ssDNA and partly dsDNA can be fit to a linear combination of ssDNA and dsDNA stretching curves[6]. Thus, the progress of DNAp can be followed by the number of single-stranded bases, N_{ss}, remaining in the template at time t

$$N_{ss}(t) = \frac{x_{meas}(F, t) - x_{ds}(F)}{x_{ss}(F) - x_{ds}(F)} * N_{tot} \qquad (1)$$

where x_{meas} is the end-to-end distance of the molecule at force F; $x_{ds,ss}(F)$ are the end-to-end distances of fully double- or single-stranded DNA at that force, and N_{tot} is the total number of bases in the template.

Figure 2a (upper line) plots the ssDNA fraction remaining at time t as DNAp replicates against an applied tension of 20 pN. The instantaneous polymerization rate (lower line) determined from the time derivative of this curve shows bursts of activity. Two lines of evidence suggest that each burst corresponds to a DNAp molecule loading onto the 3′ end of the growing chain, replicating proces-
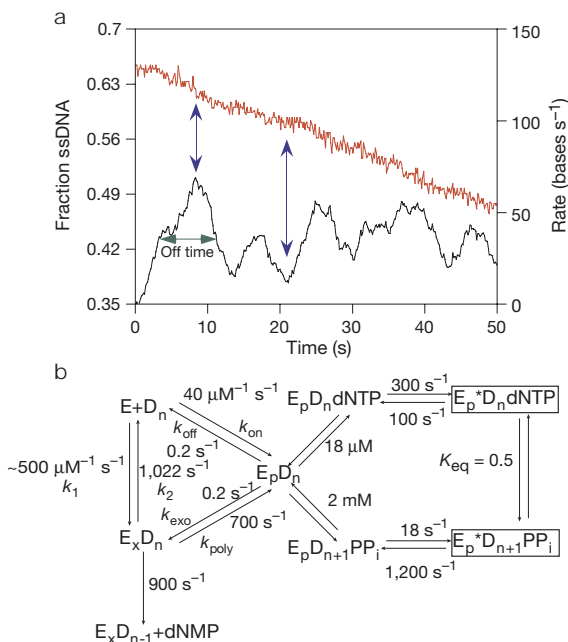
sively, and falling off. First, the mean width of a burst is force and concentration independent, and the rate corresponding to this width (0.13 ± 0.1 s⁻¹; N = 62) is near the off rate from the polymerization site measured in bulk[9]. Second, varying the DNAp concentration changed the width of the gaps between bursts. At 0.8 nM, gap widths average 7 ± 4 s, consistent with ~7 s calculated from the enzyme loading rates from solution (~180 s⁻¹ μM⁻¹; Fig. 2b). Increasing the DNAp concentration to 8 nM, decreased gap size to 1.7 ± 0.8 s. At 80 nM and 880 nM, however, this trend reversed and the gaps increased to 7 ± 2 s and 50 ± 26 s, respectively. Notably, T7 DNAp can bind non-specifically along ssDNA with a dissociation constant of ~800 nM[10]. Therefore, such binding may block enzyme reloading at the 3′ end, increasing gap widths. Because the average burst height remained independent of enzyme concentration (data not shown), non-specific binding does not seem to impede translocation once an enzyme is specifically bound. Occasionally, replication would stop for extended periods (up to 30 min), indicating 'roadblocks' that the polymerase would not cross. Causes might include exogenous DNA hybridized to the template or bases missing from the template because of chemical or enzymatic damage. Template hairpins are an unlikely cause as blockage persists above 15 pN, where such structures should pull out[11].

Figure 2a shows surprising diversity in polymerization rates among individual DNAp molecules. Burst heights typically vary between 26 and 60 bases s⁻¹ (N = 39, s.d. = 17), at a template tension of 20 pN. As the intrinsic rate of each DNAp molecule can be determined from analysis of burst heights (see Methods), such variations probably reflect differences in enzymatic activity among individual molecules. Similar differences have been reported for other enzymes[12,13].

The effect of template tension on the polymerization rate was determined either by holding the tension constant through force-feedback or by holding the template strand at constant end-to-end length. This length was chosen beyond the crossover point, so that polymerization increased template tension until the system halted itself, having sampled all intermediate tensions (Fig. 3). At the lowest tension, the replication rate of T7 DNAp was ~100 bases s⁻¹. Raising template tension increased the replication rate until a maximum of ~200 bases s⁻¹ was reached at about 6 pN. Further increase in tension, however, caused the rate to decrease until polymerization stalled. For 12 constant-distance runs, the mean stall force was 34 ± 8 pN. On rare occasions, polymerization

Figure 2 Polymerization kinetics. **a**, Replication of a ssDNA template under 20 pN tension using 8 nM DNA. Upper curve, conversion to dsDNA plotted as fraction of ssDNA left in the template versus time. Lower curve, polymerization rate obtained by differentiating upper curve after smoothing it with a moving-average filter (24 data points) to reduce Brownian noise. **b**, Induced fit kinetic pathway of T7 DNAp according to Patel *et al.*[9] with k_1 and k_2 taken from Donlin *et al.*[16]. States of the DNA–enzyme complex are shown as: E, enzyme in solution; $E_{p,x}$, DNA bound in polymerase active site or exo active site; D_n, DNA primer with length n; dNTP, deoxynucleotide; and PP_i, pyrophosphate.
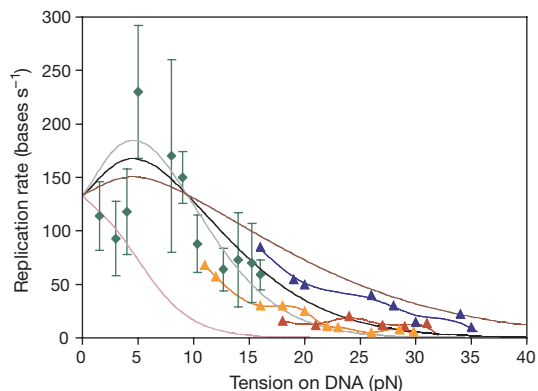
Figure 3 Polymerization rate versus template tension. Diamonds represent 50 polymerization bursts taken at 11 different tensions (error bar, s.d.); triangles represent three traces fitted through a succession of replication bursts measured at constant end-to-end distances until a stalling force in reached; thick lines represent fits of equation (4) using $a = 0$, $k_0 = 130$ bases s⁻¹, and $n = 1$ (brown), $n = 2$ (black), $n = 3$ (grey) and $a = 1$ nm, $n = 2$ (purple). Noise increases near 0 pN and the crossover point, because the numerator and denominator of equation (1) become small while the brownian motion does not decrease.

proceeded briefly above 50 pN. Replication did not restart spontaneously at these high tensions even after several minutes, but replication always resumed after lowering the tension. The force would then rise once again until a new stalling force, usually different from the previous one, was reached, perhaps reflecting the effect of template sequence, or the stochastic nature of the stalling process itself.

The sensitivity of the polymerization rate even to low tensions indicates that the rate-limiting step is directly affected by force. This force dependence is consistent with the induced-fit model of Wong *et al.*[14], in which the enzyme changes conformation during the rate-limiting step. Crystal structures of the closed state show the fingers rotated ∼40° to align the different components in the active site[3,4], and the ssDNA bending sharply in relation to the primer as it leaves this site.

If the tension, F, on the template can exert a torque on the fingers, the work done by the enzyme would include a term aF, where a is the distance moved by the fingers along the pulling direction of the template. Further, assume that closing the fingers organizes n adjacent sugar-phosphate units from single- to double-stranded geometry, $n - 1$ of which are released when the fingers reopen. Then the work W to close the fingers is

$$W(F) = aF + nF(x_{ss}(F) - x_{ds}(F)) \qquad (2)$$

where $x_{ss}(F)$ and $x_{ds}(F)$ are the end-to-end distances per base of ssDNA and dsDNA at tension F. The second term in equation (2) changes sign at 6.5 pN, aiding or opposing replication below or above this force and causing the instrument to do work on the reaction or the reaction to do work on the instrument, respectively. Closing of the fingers also clamps the template strand reducing its degrees of freedom. Tensions applied to the template decrease its entropy and, consequently, the energetic cost of closing the fingers, thus speeding up the reaction. The entropy change, ΔS, to convert ssDNA into dsDNA at any given force can be obtained from the areas under the experimental force–extension curves (Fig. 1b), that is,

$$T\Delta S(F) = n\left[\int_0^{x_{ss}(F)} F_{ss}\,dx - \int_0^{x_{ds}(F)} F_{ds}\,dx \right] \qquad (3)$$

where $F_{ds,ss}$ are the experimental forces required to extend the chains by an amount x. If we assume that the terms in equations (2) and (3) contribute to the activation energy required to reach a transition state (for example, the complex with fingers half-closed) from the open state, then the rate coefficient (k) for this step is

$$k = k_0 e^{-((w - T\Delta S)/k_b T)} \qquad (4)$$

where k_o is the rate coefficient at zero force; k_b is the Boltzman constant and T is the temperature. Figure 3 compares equation (4) to the data using various values of a and n. The best fit is obtained for $a = 0$ and $n = 2$, indicating that template tension exerts little torque opposing finger closure and that two adjacent sugar-phosphate units are organized by the fingers in this process. These results are supported by the structure of the closed complex which shows the template strand avoiding the finger tips and passing around the side of the fingers through a shallow cleft[3,4]. Moreover, two adjacent template bases appear immobilized in this structure. The first, opposite the incoming nucleotide, adopts a B-form structure, whereas the second is kinked outward, almost perpendicular to the pulling direction. The interphosphate distance corresponding to these two bases is close to that of dsDNA. Subsequent bases ($n > 2$) appear disorganized in the structure. Single-molecule studies of an exonuclease-deficient mutant of T7 DNAp (Sequenase) also suggest immobilization of two bases during finger closure (B. Maier, D. Bensimon and V. Croquette, personal communication).

When template tension was increased above 40 ± 3 pN ($N = 16$), a fast exonucleolysis (30 ± 11 bases s[−1]) was initiated with or
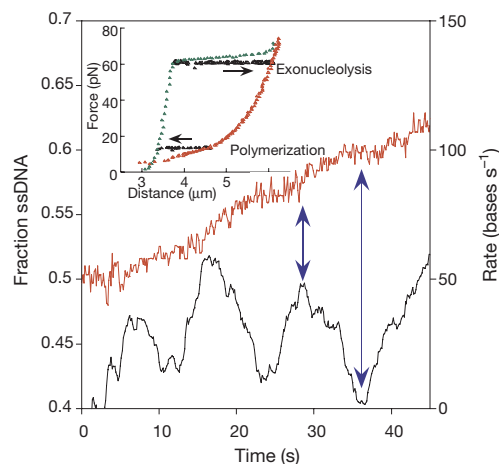

Figure 4 Exonuclease digestion of primer strand by T7 DNAp (at 8 nM) at template tension of 50 pN. Upper curve, ssDNA fraction of 10-kilobase template. Lower curve, exonuclease rate obtained by differentiating upper curve after application of a 3-s moving-average filter. Inset, force–extension curve for a dsDNA molecule (green points) before it was almost entirely converted to ssDNA by exonucleolysis at a constant force of 60 pN (upper horizontal points, right arrow). At the end of this process a force-extension curve for the ssDNA was obtained (red points). Finally, in the presence of dNTPs, the tension was decreased to 15 pN to allow T7 DNAp to reconvert ssDNA into dsDNA (lower horizontal points, left arrow).

without dNTPs present (Fig. 4). Decreasing tension below ∼34 pN caused exonucleolysis to halt and polymerization to resume. Switching between these opposite activities (inset, Fig. 4) could be repeated many times on one template (data not shown). Exonucleolysis force dependence was measured either using constant force or constant end-to-end distance (Fig. 5). The exonucleolysis rate became force independent above 42 pN and is ∼100 times faster than observed at zero tension on dsDNA, where the exo rate is limited by the escape of the 3′ end from the polymerization site (Fig. 2b). Force-induced exonucleolysis appears as bursts of activity (Fig. 4, lower line). Presumably, template tension shifts the equilibrium in favour of exonucleolysis either by increasing the escape rate from (k_{off} and k_{exo}) or decreasing the binding rate to (k_{on} and k_{poly}) the polymerization site, or both. However, if the escape rate from the polymerization site were increased by two orders of magnitude, such escape would still be rate limiting for exonucleolysis ($0.2\,s^{-1} \times 100$) which would appear continuous at our temporal resolution. The gaps observed in the exonuclease rate are instead consistent with a 100-fold decrease in binding rate to the polymerization site. Because the enzyme bound through its exonuclease site associates/dissociates rapidly from solution to the 3′ end (Fig. 2b), many DNAps can bind, exonucleate and dissociate, before one of them moves back to the polymerase site. It then takes several seconds for this enzyme to escape the polymerase site ($k_{exo} = 0.2\,s^{-1}$), resulting in gaps of activity as observed in Fig. 4. Thus, each exo-pause results from one DNAp molecule lingering in the polymerization active site, while each exo-burst, seeming continuous because of our temporal resolution, could result from the action of many individual DNAp molecules.

Although the gaps can be explained by a slow escape of the 3′ end from the poly site, the heights of the exo-bursts are inconsistent with published association/dissociation rates of the exo site from solution (k_1 and k_2, Fig. 2b). Unexpectedly, the forced-induced exonucleolysis rate remains relatively constant for DNAp concentration between 800 nM and 8 nM, dropping by 50% only when the concentration is lowered to 0.8 nM. Under zero tension, it is thought that several base pairs must be melted to allow binding of the DNA primer strand to the exonuclease site[5], and forces greater
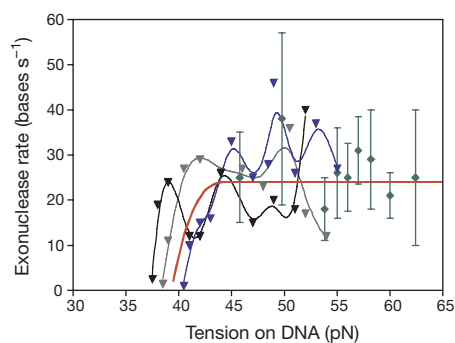
Figure 5 Force dependence of $3' \rightarrow 5'$ exonuclease reaction. Diamonds represent average rates for 49 (total) exonuclease bursts measured at 9 different forces. Traces represent three lines fitted through successions of exonucleolysis burst heights (triangles), initiated at high tensions, on DNAs kept at constant end-to-end distances. Digestion lowers the tension in the DNA until the fast exonucleolysis stops. The upper limit for these experiments is determined by the overstretching force, 65 pN[6,19]. Near the stalling force for polymerization, a competition was occasionally observed between exonucleolysis and polymerization which caused the template tension to bounce up and down every few seconds.

than 40 pN are known to promote fraying in dsDNA[15]. Perhaps the exonucleolysis rates simply reflect the rate of fraying of DNA at the tensions applied to the template and the known fast exo activity of T7 DNAp[16] on ssDNA. To test this idea, we investigated the effect of template tension on the activity of *Escherichia coli* exonuclease I. This enzyme attacks only ssDNA[17] at its $3'$ end, so it should not digest the primer strand unless it frays. No activity was detected under a tension of 40 pN, but at 50 pN bases were removed at a rate of $\sim 200\ s^{-1}$. This fast exonucleolysis suggests that $3'$ end fraying is not rate limiting during exonucleolysis by T7 DNAp. Thus, the force-induced exonucleolysis initiated at 40 pN is probably a specific property of T7 DNAp itself. For example, 40-pN tension may deform the dsDNA geometry at the $3'$ end enough to trigger the enzyme's proof-reading function. But, as Fig. 5 shows, the fraying is rate limited in the presence of T7 DNAp. Perhaps the melting rate is mediated by some interaction with the enzyme which is independent of the tension. Future single-molecule experiments should elucidate the mechanism of force-induced exonucleolysis and provide additional insight into the mechanochemistry of DNA polymerase. □

Methods

Single-molecule assay

T7 DNAp (T7 gene 5 in a 1:1 complex with thioredoxin) was used in various concentrations (0.8–880 nM), where 1 nmol = $\sim$230 activity units (Amersham). Replication buffer was 40 mM Tris pH 7.5, 5 mM MgCl$_2$, 50 mM NaCl, 50 μg ml^{-1} BSA, 0.1% NaN$_3$, 5 mM dithiothreitol and 0.6 mM (each) dNTPs. The end of one of the DNA chains was covalently coupled to a bead while the other end of the same chain was attached through a biotin/streptavidin linkage to the second bead[18] (Fig. 1a). Exonuclease I (USB) was used at 50 units ml^{-1} in replication buffer altered to pH 8 and without dNTPs.

Temporal resolution

Data were collected at 8 Hz with a bandwidth of 60 Hz. The polymerization rate data was averaged over 3 s and, therefore, the height of bursts longer than 3 s should represent the intrinsic activity of individual molecules. For the expected average replication time ($\sim$5 s), most burst heights will be accurately determined with this temporal resolution. No correlation between burst height and width (measured at the half maximum) was found for bursts longer than 3 s.

Processivity

Because the replication rate varies with force (Fig. 3), whereas the dissociation rate (k_{off}) seems to remain constant, the processivity varies with force and is $\sim$420 bases (60 bases s^{-1}, 0.13 s^{-1}) at 15 pN.

1. Modrich, P. & Richardson, C. C. Bacteriophage T7 deoxyribonucleic acid replication *in-vitro*. Bacteriophage T7 DNA polymerase: an enzyme composed of phage- and host-specific subunits. *J. Biol. Chem.* **250**, 5515–5522. (1975).
2. Tabor, S., Huber, H. E. & Richardson, C. C. *Escherichia coli* thioredoxin confers processivity on the DNA polymerase activity of the gene 5 protein of bacteriophage T7. *J. Biol. Chem.* **262**, 16212–16223 (1987).
3. Doublie, S. & Ellenberger, T. The mechanism of action of T7 DNA polymerase. *Curr. Opin. Struct. Biol.* **8**, 704–712 (1998).
4. Doublie, S. *et al.* Crystal structure of a bacteriophage T7 replication complex at 2.2 Å resolution. *Nature* **391**, 251–258 (1998).
5. Johnson, K. A. conformational coupling in DNA polymerase fidelity. *Annu. Rev. Biochem.* **62**, 685–713 (1993).
6. Smith, S. B., Cui, Y. & Bustamante, C. Overstretching B-DNA: the elastic response of individual double-stranded and single-stranded DNA molecules. *Science* **271**, 795–799 (1996).
7. Marko, J. F. & Siggia, E. D. Stretching DNA. *Macromolecules* **28**, 8759–8770 (1995).
8. Bustamante, C., Marko, J. F., Siggia, E. D. & Smith, S. B. Entropic elasticity of lambda-phage DNA. *Science* **265**, 1599–1600 (1994).
9. Patel, S. S., Wong, I. & Johnson, K. A. Pre-steady-state kinetic analysis of processive DNA replication including complete characterization of an exonuclease-deficient mutant. *Biochemistry* **30**, 511–525 (1991).
10. Huber, H. E., Tabor, S. & Richardson, C. *Escherichia coli* thioredoxin stabilizes complexes of bacteriophage T7 DNA polymerase and primed templates. *J. Biol. Chem.* **262**, 16224–16232 (1987).
11. Essevaz-Roulet, B., Bockelmann, U. & Heslot, F. Mechanical separation of the complementary strands of DNA. *Proc. Natl Acad. Sci. USA* **94**, 11935–11940 (1997).
12. Xue, Q. & Yeung, E. Differences in the chemical reactivity of individual molecules of an enzyme. *Nature* **373**, 681–683 (1995).
13. Lu, H. P., Xun, L. & Xie, X. S. Single-molecule enzymatic dynamics. *Science* **282**, 1877–1882 (1998).
14. Wong, I., Patel, S. S. & Johnson, K. A. An induced-fit kinetic mechanism for DNA replication fidelity: direct measurement by single-turnover kinetics. *Biochemistry* **30**, 526–537 (1991).
15. Gurrieri, S., Smith, S. B. & Bustamante, C. Trapping of megabase-sized DNA molecules during agarose gel electrophoresis. *Proc. Natl Acad. Sci. USA* **96**, 453–458 (1999).
16. Donlin, M. J., Patel, S. S. & Johnson, K. A. Kinetic partitioning between the exonuclease and polymerase sites in DNA error correction. *Biochemistry* **30**, 538–546 (1991).
17. Lehman, I. R. & Nussbaum, A. L. On the specificity of *E-coli* exonuclease I. *J. Biol. Chem.* **239**, 2628–2636 (1964)
18. Hegner, M., Smith, S. B. & Bustamante, C. Polymerization and mechanical properties of single RecA-DNA filaments. *Proc Natl Acad. Sci. USA* **96**, 10109–10114 (1999).
19. Cluzel, P. *et al.* DNA: an extensible molecule. *Science* **271**, 792–794 (1996).